Střelcová, K., Škvarenina, J. & Blaženec, M. (eds.): **"BIOCLIMATOLOGY AND NATURAL HAZARDS"**
International Scientific Conference, Poľana nad Detvou, Slovakia, September 17 - 20, 2007, *ISBN 978-80-228-17-60-8*

Dual-continuum modeling of dye tracer infiltration into soil with biopores

M. Dohnal [(1)], J. Dušek [(1)], T. Vogel [(1)], M. Císlerová [(1)], Ľ. Lichner [(2)] and V. Štekauerová [(2)]

[(1)] Czech Technical University, Faculty of Civil Engineering, Thakurova 7, 166 29 Prague, Czech Republic
(e-mail: dohnalm@mat.fsv.cvut.cz)
[(2)] Institute of Hydrology, Slovak Academy of Sciences, Racianska 75, 831 02 Bratislava, Slovak Republic

Abstract Adequate modeling of infiltration into heterogeneous structured soils from ponded sources represents an important scientific problem with numerous implications for practical hydrological tasks, e.g. estimation of irrigation demand, runoff prediction and contaminant transport in the vadose zone. Reliable predictions of the three-dimensional flow of water are often complicated by the presence of preferential pathways. The present study is focused on numerical modeling of a field infiltration experiment. The experiment involved ponded infiltration from a single infiltration ring into the soil profile containing biopores (Calcari-Haplic Chernozem, Macov station, Danubian Lowland, Slovak Republic). The presence of biopores network in the soil of interest was proved by the accompanying tracer experiment. To quantify the preferential flow effects, numerical model based on the dual-continuum approach was employed. The spatial distribution approximate volumetric fraction of the preferential pathways were evaluated by means of digital image analysis. The results provide valuable information about the movement of water through soils with biopores.

Key words: *vadose zone, infiltration, tracer experiment, dual-continuum model, preferential flow, biopores*

Introduction

Although macropores usually occupy relatively small volume of bulk soil, they may significantly change water flow patterns and transport of pollutants. Preferential flow in macropores often significantly enhances infiltration into soils. Detailed knowledge of water flow through preferential pathways is of a major importance when predicting rainfall-runoff responses of catchments. In the 19th century, the hydrologists widely speculated about the role and effects of soil bypassing and channeling on water regime while more sophisticated attention received a phenomenon of flow in macropores at the end of the 20th century (e.g. Beven and Germann 1982, Hole 1981). Preferential flow in soils may be triggered by a variety of causes. Biopores as a result of fauna and flora abundance are quite difficult to quantify. Process of water flow through natural biopores and its consequences for infiltration have been evaluated e.g. by Leonard and Rajot (2001). Moreover, biopores may be enriched with organic carbon and biomass which suggests notable impact on solute transport in porous media. Peyton et al. (1992) used X-ray tomography to quantify the macropore diameter in undisturbed soil sample. They found the diameter of a single macropore in range from 0.5 to 1 mm. Weiler and Naef (2003), among others, focused on macropores which are active during the infiltration process by applying a conservative tracer.

The water repellency of soils may be another reason for the onset of preferential flow. In this case, infiltrated water is channeled in active flow area while other portion of soil stays dry due to repellency and low local hydraulic conductivity (Ritsema et al. 1993). As a result, the infiltration process exhibits great variability in both space and time. Hence, more attention should be paid also to the time variability of infiltration in natural systems. One of the most important phases of infiltration is its early stage (Zhou et al. 2002). The infiltration variability may be even increased by the air entrapment in soils. These effects are usually accompanied by an occurrence of air bubbles in an infiltration ring during infiltration experiment. At the very beginning of infiltration, a relatively small increase of air pressure below the wetting front may cause a drastic decrease of infiltration rate (by factor of 3 up 10). In addition, air entrapment together with soil repellency may lead to fingering effects and flow instabilities (Wang et al. 1998).

From the above mentioned aspects, it is clearly evident that numerical simulation of infiltration into macroporous soils poses a definite challenge. The simplifying assumptions involved in currently available models are rarely perfectly satisfied, which leads to large uncertainties in model predictions. There are different approaches how to address the difficult task of modeling infiltration into macroporous soil. These approaches range from a simple one-dimensional algebraic infiltration model with only three fitting parameters (Wang et al. 2003) to more sophisticated approaches such as axisymmetric linear two-phase flow model (Felton and Reddell 1992) or model for simulating infiltration through clay segments (Bundt et al. 2001). A higher level of complexity is achieved by the dual porosity (Gerke and van Genuchten 1993a) and kinematic wave-based (Jarvis 1994) approaches. However, mutual comparison of the model performance of these two approaches in particular case studies has shown ambiguous results (Simunek et al. 2003).

The objective of this study is (i) to give experimental evidence about preferential movement of water in Chernozem soil, (ii) to apply the inverse modeling to minimize discrepancies between model responses and observations, and (iii) to present numerical simulations

of infiltration into macroporous soil with 3D dual-permeability approach.

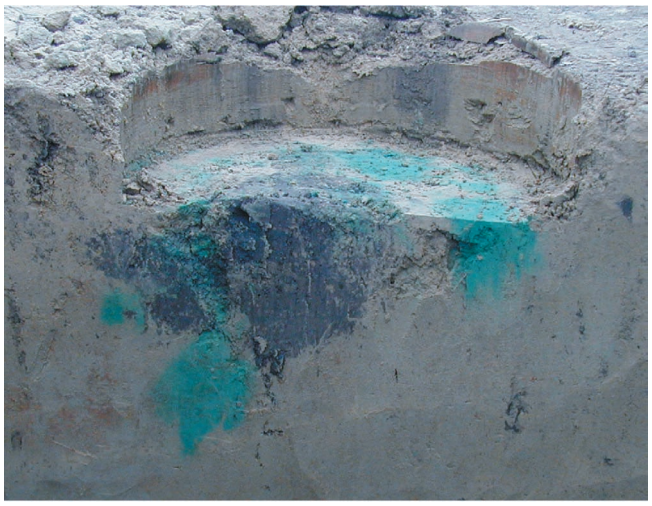

Fig. 1 The soil profile below excavated infiltration ring

Material and methods

The soil and experiments

One of the objectives of this paper is the identification of the character of water infiltration into soil in Danubian Lowland (Slovak republic). The soil in the area of interest is being intensively used in agriculture. The soil at experimental station Macov is, from the point of view of texture, graded as medium heavy loamy soil and is classified as Calcari-Haplic Chernozem according to soil database (WRB 1998). The soil is underlain with carbonate bedrock. The water table resides at about 6 m below the soil surface, thus it did not influence the conducted experiments.

Ponded infiltration experiments were performed at several locations at Macov station. Since the individual infiltration runs did not vary significantly from each other, one infiltration experiment was chosen and is assumed to be representative for the whole site in the following paragraphs. The steel infiltration ring provided infiltration area of 1000 cm^2. It was carefully pushed 15 centimeters into the soil profile in order to avoid boundary effects along the wall. The grass vegetation was left intact inside the ring during the experiment. During the first stage of the infiltration experiment, 21 cm of clean water was allowed to infiltrate into the soil profile for 110 min (when quasi steady state flow conditions were reached) by supplying periodically small doses of water (to keep the water level in the infiltration rings at an approximately constant level). Then, Brilliant Blue tracer was added to the infiltration ring dissolved in the last dose of water. After the cessation of water supply, the soil profile was cautiously excavated and the penetration depth of the applied tracer was recorded by a digital camera. In addition, one ponded infiltration experiment was carried out on deeper soil horizon, at 70 cm below the soil surface (at different location). During the soil excavation, the abundance of biopores either as a product of fauna (earthworms, ants etc.) or flora (decayed roots) was markedly visible (Fig. 1). The network of biopores was found to be highly irregular in the whole profile. It reached down to 150 cm below the surface where the excavation was stopped. The top soil was partly fissured after prolonged rainless period.

The spatial distribution of the dye-stained area together with the depth of tracer penetration was obtained by the gradual excavation of the soil profile. Photographs of the tracer penetration were taken in a sequence of horizontal cross-sections (a few centimeters apart) along the vertical axis.

The retention curves were determined from the laboratory measurements for four soil horizons. Each layer was represented by at least three replicates. The hydraulic parameters (Tab. 1) were derived from the relationship between measured water content and respective pressure head using modified van Genuchten's model (Vogel et al. 2001). Relatively slight differences of hydraulic parameters among the individual soil horizons indicate nearly homogeneous soil profile (from the hydrological point of view). Nevertheless, at the depth of 60 cm, there is a distinct interface between two soil horizons. The saturated hydraulic conductivity determined from the steady state phase of ponded infiltration experiments was in close agreement with previous measurements (Lichner and Houskova 2001). Estimation of hydraulic parameters (Tab. 2), characterizing the domain of biopores, was based on the assumption that the pathways were completely filled with a coarse textured porous material.

Numerical model

The mathematical modeling comprised of three-dimensional axisymmetric simulations carried out by a two-dimensional dual-permeability code S2D (Vogel et al. 2000). The entire pore space is represented by a dual-continuum system (Gerke and van Genuchten 1993a). The dual-permeability concept assumes Richards' type flow in two mutually communicating pore domains – the soil matrix (MF-domain, subscript *m*) and preferential flow domain (PF-domain, subscript *f*). Preferential flow domain occupies only a certain fraction of the bulk soil. The modified van Genuchten approach (Vogel et al. 2001) was used for the parameterization of unsaturated hydraulic conductivity function.

Assuming radial coordinate system water flow in a dual-permeability porous medium is described by a pair of Richards' equations

$$C_m \frac{\partial h_m}{\partial t} = \nabla \cdot \left(\mathbf{K}_m \nabla h_m\right) + \nabla \cdot \left(\mathbf{K}_m \nabla z\right) + \frac{\Gamma_w}{w_m} \qquad (1)$$

$$C_f \frac{\partial h_f}{\partial t} = \nabla \cdot \left(\mathbf{K}_f \nabla h_f\right) + \nabla \cdot \left(\mathbf{K}_f \nabla z\right) - \frac{\Gamma_w}{w_f} \qquad (2)$$

where h represents the pressure head [L], **K** is the hydraulic conductivity tensor [LT^{-1}], C the specific hydraulic capacity [L^{-1}], z the vertical coordinate taken positive upward, t denotes time [T], w_f is relative volumetric proportion of the preferential domain, $w_m = 1 - w_f$, and Γ_w is the water transfer term [T^{-1}]. This term mediates the exchange of water between both pore domains. The water exchange is directly proportional to pressure head difference between the matrix and preferential domains

$$\Gamma_w = \alpha_w (h_f - h_m) \quad (3)$$

where α_w is the water transfer coefficient [$L^{-1}T^{-1}$] for which Gerke and van Genuchten (1993b) used following semi-empirical formula

$$\alpha_w = \gamma_w \frac{\beta}{a^2} K_a \quad (4)$$

in which a is the characteristics length [L], β denotes dimensionless geometric coefficient [-] and, K_a is the hydraulic conductivity at the matrix-macropore interface [LT^{-1}]. K_a function and its characteristics are adopted from work of Ray et al. (2004). γ_w (= 0.4) is an empirical scaling factor of Gerke and van Genuchten (1993a,b; 1996).

Numerical experiments

The axisymmetric flow domain has a cylindrical shape (2 m in diameter and 1.5 m deep) concentric with the infiltration ring. The finite element mash is made finer near the soil surface where steep wetting front develops. According to the field experiment, the depth of insertion of the infiltration ring is considered to be 15 cm. The volumetric portion of the PF-domain is estimated from the image analysis to be 7% of the bulk soil.

During the whole simulation period, the water level in the infiltration ring was kept 3 cm above the soil surface thus resulting in the constant pressure boundary condition. The lower boundary of the simulated domain was treated as the unit hydraulic gradient boundary. Zero-flux condition was imposed on all remaining boundaries. At the beginning of the simulation period, equilibrium state with groundwater table at 600 cm below the soil surface was applied as initial condition.

The associated inverse problem was solved by Levenberg-Marquardt nonlinear optimization method (Doherty et al. 1995). The hydraulic parameters were optimized by means of the least square method.

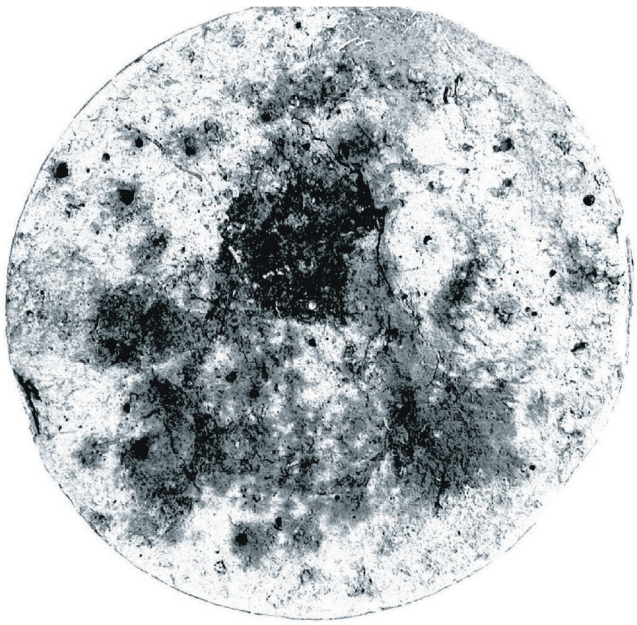

Fig. 2 The excavated cross-section just below the infiltration ring. Black spots near the centre are related to organic matter. Dark gray spots represent saturated soil. At this level, less than half of the area conducted water during the infiltration experiment.

Table 1 Measured hydraulic parameters for the soil matrix domain

layer number	depth (cm)	layer thickness (cm)	θ_r (-)	θ_s (-)	α (1/cm)	n (-)	K_s (cm/d)
1	0-25	25	0.000	0.498	0.018	1.212	24.0
2	25-60	35	0.000	0.494	0.050	1.180	18.0
3	60-80	20	0.000	0.452	0.026	1.215	10.0
4	80-150	70	0.000	0.479	0.016	1.647	10.0

Table 2 Hydraulic parameters for the preferential flow domain

layer number	depth (cm)	layer thickness (cm)	θ_r (-)	θ_s (-)	α (1/cm)	n (-)	K_s (cm/d)
1÷4	0÷150	150	0.050	0.430	0.145	2.680	2400

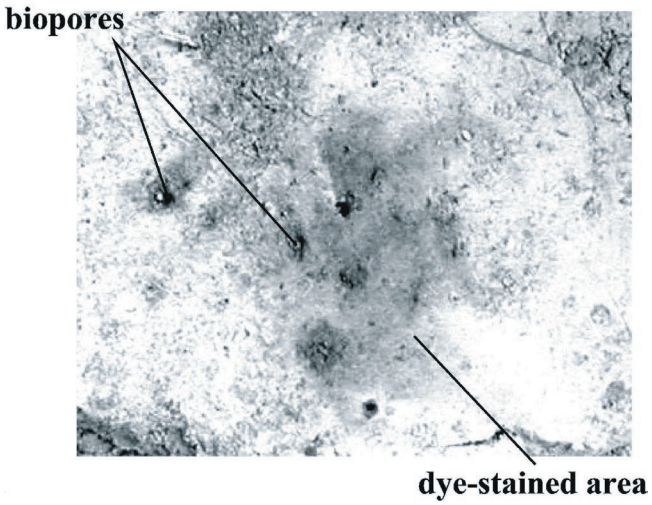

Fig. 3 The picture shows close-up of the excavated soil plane at the depth of 60 cm below the soil surface. A few macropores mostly related to root system continue from higher soil horizons.

Results and discussion

Fig. 2 shows the excavated soil section just below the experimental infiltration ring. Few biopores are easily visible with the naked eye. These biopores originated from an abundance of earthworms. Several biopores are as wide as a few millimeters in diameter. As could be expected, most biopores conducted the dye tracer. An organic soil lens of dark color can be seen in the center of the soil section. This part of the section also significantly contributed to water flow. Stained areas near the larger pores indicate diffusion of water.

Strongly preferential character of water flow is demonstrated in Fig. 3. The close-up of the excavated soil surface at the depth of 60 cm clearly shows macropores conducting water/tracer from higher soil horizons.

In order to minimize discrepancies between the simulated and measured cumulative infiltration data, acquired during the transient infiltration experiment, inverse parameter estimator was used. The parameters listed in Tab. 1 and Tab. 2 for the soil matrix and PF-domain, respectively, served as initial estimates for inverse modeling. First, the soil matrix parameters determined at the laboratory scale were upscaled to the field scale by means of scaling factors of pressure head, hydraulic conductivity and water content (Vogel et al. 1991). Then only the first layer soil matrix parameters α, n, and K_s were optimized. The remaining parameters were fixed to their initial estimates. The volumetric fraction of the preferential pathways was estimated from the image analysis of the tracer experiment.

The simulated infiltration rates are shown in Fig. 4. The results obtained from the inverse modeling contributed notably to closer agreement between measured and simulated infiltration rate and provided valuable information about water movement through the soil profile under field conditions.

The conducted 3D axisymmetric simulations provided the time development of the soil water pressure below the infiltration ring. The simulated depth of penetration after nearly 2 hours of continuous water supply was relatively close to the observed one. The results of the 3D axisymmetric dual-permeability simulation are shown in Fig. 5. Note the sharp wetting front in the PF-domain (Fig. 5b). In case that the preferential flow effects are neglected, much poorer agreement between the simulated and measured penetration is obtained. Specifically, single-continuum model failed to predict the observed dye penetration beyond the depth of 60 cm.

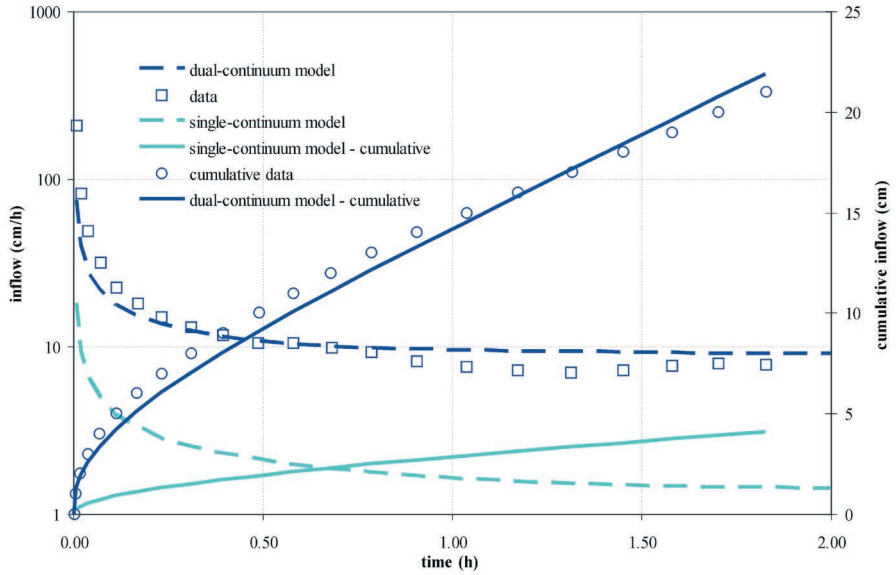

Fig. 4 Measured and simulated infiltration rates

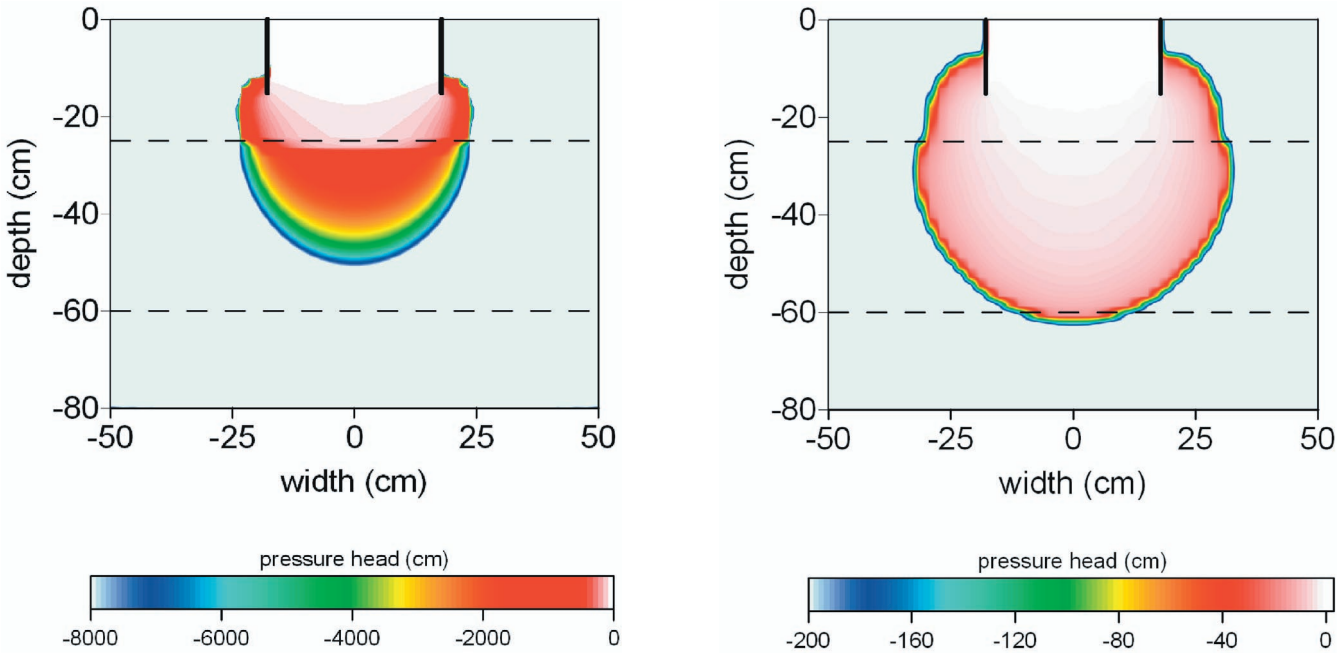

Fig. 5 Simulated pressure head profiles in the matrix domain (a), and the PF-domain (b) at 110 min after the beginning of the infiltration experiment.

Conclusions

As mentioned earlier in the introductory part, modeling of infiltration into macroporous soils does not represent a trivial problem. Nevertheless, with help of numerical modeling, quite reliable space time information about the soil water flow during infiltration can be obtained.

The presence of preferential flow paths in a lowland agricultural soil was demonstrated by means of a dye-tracer infiltration experiment. The dye tracer experiment helped to identify the active flow regions in the soil under study.

The 3D axisymmetric simulation based on dual-permeability approach provided relatively realistic space-time distribution of soil water pressure below the infiltration ring. Moreover, the simulated wetting front position after 110 minutes of continuous water supply indicates quite good agreement with the measured tracer penetration. Water flow simulation, based on measured hydraulic characteristics without consideration of preferential flow effects does not describe the infiltration experiment adequately.

Acknowledgement

The research has been supported by the European Union FP6 Integrated Project AquaTerra (Project no. 505428) under the thematic priority "sustainable development, global change and ecosystems", and by the Research Center "CIDEAS" of the Ministry of Education of the Czech Republic. Additional funding has been provided by the Slovak Scientific Grant Agency VEGA Project 2/6003/26.

References

[1] Beven K.J., Germann P. (1982): Macropores and water flow in soils. Water Resources Research, *18:* 1311–1325.

[2] Bundt M., Widmer R., Pesaro M., Zeyer J., Blaser P. (2001): Preferential flow paths: biological 'hot spots' in soils. Soil biology & Biochemistry, *33:* 729-738.

[3] Doherty, J., Brebber L., Whyte P. (1995): PEST. Model Independent Parameter Estimation, Australian Centre for Tropical Freshwater Research, James Cooke University, Townsville, Australia.

[4] Felton G.K., Reddell D.L. (1992): A finite element axisymetrical and linear-model of 2-phase flow through porous media. Transactions of the ASAE, *35:* 1419-1429.

[5] Gerke H.H. and van Genuchten M.Th. (1993a): A dual-porosity model for simulating the preferential movement of water and solutes in structured porous media. Water Resources Research, *29***:** 305–319.

[6] Gerke, H. H. and van Genuchten M.Th. (1993b): Evaluation of a first-order water transfer term for variably saturated dual-porosity models. Water Resources Research, *29:* 1225–1238.

[7] Gerke H.H. and van Genuchten M.Th. (1996): Macroscopic representation of structural geometry for simulating water and solute movement in dual-porosity media. Advances in Water Resources, *19:* 343–357.

[8] Hole F.D. (1981): Effects of animals on soils. Geoderma, *25*: 75-112.

[9] Jarvis N. (1994): The MACRO Model (Version 3.1). Technical description and sample simulations. Reports and dissertations No. 19, Uppsala, 51 pp.

[10] Leonard J., Rajot J.L. (2001): Influence of termites on runoff and infiltration: quantification and analysis. Geoderma, *104:* 17-40.

[11] Lichner Ľ., Houšková B. (2001): Časová variabilita hydraulickej vodivosti pôd s makropormi. Acta Hydrologica Slovaca, *2*: 1-8.

[12] Peyton R.L., Haeffner B.A., Anderson S.H., Gantzer C.J. (1992): Applying X-ray CT to measure macropore diameters in undisturbed soil cores. Geoderma, *53:* 329-340.

[13] Ray C., Vogel T., Dusek J. (2004): Modeling depth-variant and domain-specific sorption and biodegradation in dual-permeability media. J. Contam. Hydrol., *70:* 63-87.

[14] Ritsema C.J., Dekker L.W., Hendrickx J.M.H., Hamminga W. (1993): Preferential flow mechanism in a water repellent sandy soil. Water Resources Research, *29:* 2183-2193.

[15] Simunek J., Jarvis N.J., van Genuchten M.Th., Gärdenäs A. (2003): Review and comparison of models for describing non-equilibrium and preferential flow and transport in the vadose zone. Journal of Hydrology, *272:* 14-35.

[16] Vogel T, van Genuchten M.Th., Císlerová M. (2001): Effect of the shape of soil hydraulic functions near saturation on variably-saturated flow predictions. Advances in Water Resources, *24:* 133–144.

[17] Vogel T, Gerke H.H., Zhang R., van Genuchten M.Th. (2000): Modeling flow and transport in a two-dimensional dual-permeability system with spatially variable hydraulic properties. Journal of Hydrology, *238:* 78–89.

[18] Vogel T., Císlerová M., Hopmans J.W. (1991): Porous media with linearly variable hydraulic properties. Water Resources Research, *27:* 2735-2741.

[19] Wang D., Feyen J., van Genuchten M.Th., Nielsen D.R. (1998): Air entrapment effects on infiltration rate and flow instability. Water Resources Research, *34:* 213-222.

[20] Wang Q.J., Horton R., Shao M.G. (2003): Algebraic model for one-dimensional infiltration and soil water distribution. Soil Science, *168:* 671-676.

[21] Weiler M., Naef F. (2003): An experimental tracer study of the role of macropores in infiltration in grassland soils. Hydrological Processes, *17:* 477-493.

[22] WRB (1998): World reference base for soil resources. World Soil Resources Reports, No. 84. FAO, Rome.

[23] Zhou Q.Y., Shimada J., Sato A. (2002): Temporal variations of the three-dimensional rainfall infiltration process in heterogeneous soil. Water Resources Research, *38:* 1032.